Exploring the Use of Local Binary Patterns as Focus Measure

J. Lorenzo, M. Castrillón, J. Méndez
Institute of Intelligent Systems (SIANI)
Univ. de Las Palmas de Gran Canaria
35017 Las Palmas, Spain
{jlorenzo,mcastrillon,jmendez}@iusiani.ulpgc.es

O. Déniz
E.T.S.Ingenieros Industriales
Univ. de Castilla-La Mancha
13071 Ciudad Real, Spain
Oscar.Deniz@uclm.es

Abstract

In this work Local Binary Patterns based focus measures are presented. Local Binary Patterns (LBP) have been introduced in Computer Vision tasks like texture classification or face recognition. In applications where recognition is based on LBP, a computational saving can be achieved with the use of LBP in the focus measures. The behavior of the proposed measures is studied to test if they fulfill the properties of the focus measures and then a comparison with some well know focus measures is carried out in different scenarios.

1. Introduction

In many applications of Computer Vision, contours play an important role because they are used as features. For example in face recognition, contours define facial features as lips or iris that are involved in lip tracking or gaze detection [2, 10]. Thus, high contrast images are needed to get the best results with those methods because contours disappear as the image blurs. High contrast images are obtained when the image is focused and many methods have been proposed to implement autofocus. Most digital still cameras include autofocus, but the development of new lens technology [6] will allow to add the autofocus capability in low cost cameras such us included in laptops or cellular phones.

Automatic focusing methods fall into two main categories: active and passive systems. Active methods are based on emitting a wave in order to estimate the distance to the object of interest and consequently adjust the lens position. Passive methods estimate the position of the lens by means of finding the position where image sharpness is maximum.

Defocus images ($g(x, y)$) can be modeled with a low-pass filtering process [13].

$$g(x, y) = I(x, y) * h(x, y) \quad (1)$$

where $I(x, y)$ denotes the focus image, $h(x, y)$ denotes the Point Spread Function (PSF) of the system modeled as low-pass filter and $*$ is the convolution operator. Therefore it is necessary to compute the amount of high frequencies in the image because the focus image is the one with highest amount of high frequencies. The amount of high frequencies can be measured both in the spatial domain or in a transformed (frequency, wavelet, ...) domain. The former are more used because they can be computed very fast, however with the improvement of DSP performance the latter are being taken into account.

As mentioned above, passive autofocusing methods adjust the focus lens to maximize the high frequency components in the image. Therefore a focus value is needed to measure the amount of high frequencies in the image. As autofocusing is a long-standing topic, in the literature a wide variety of focus algorithms have been proposed each one with an associated focus measure [5, 13, 7, 18, 8, 12, 3, 17, 16, 4].

Since its introduction by Ojala [14], Local Binary Patterns (LBP) have received the attention of the Computer Vision community because they can be computed very fast and good results are obtained in problems like texture classification [14, 15], face recognition [1, 9] and iris detection [19].

In this work a novel application of Local Binary Patterns (LBP) is presented that has not been studied until now. It will be shown that LBP fulfills the properties of a focus measure. To test the goodness of LBP as a focus measure, a comparison will be carried out in different scenarios. The main goal of this work is to study if LBP based focus measures have a similar performance to other measures so an computational saving can be achieved in some applications, because with the results of the LBP computation can be solved two problems: autofocus and recognition as shown in Figure 1

This paper is organized as follows. Section 2 introduces the use of LBP as a focus measure. Section 3 explains other focus measures to be compared with LBP. Section 4 de-

978-0-7695-3514-2/08 $25.00 © 2008 IEEE
DOI 10.1109/CIMCA.2008.123

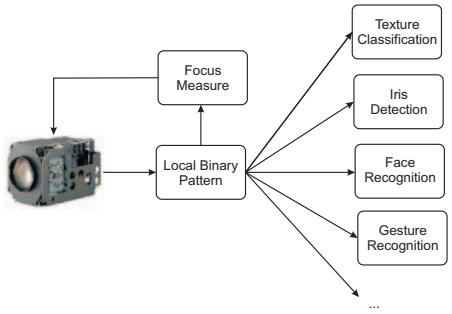

Figure 1. Local Binary Patterns as focus measure and feature for identification tasks

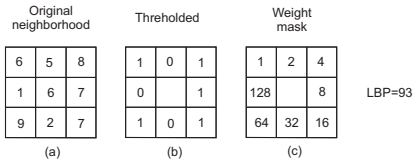

Figure 2. Local Binary Patterns

scribes the experiments and finally in Section 5 the results achieved are commented.

2 Local Binary Patterns as a focus measure

Ojala et al. [14] introduced the Local Binary Pattern texture operator shown in Figure 2. To compute the LBP operator, in each 3x3 window the neighborhood is thresholded by the value of the center pixel (Fig. 2 b). Then the value of the pixels in the thresholded neighborhood are weighted and summed to obtain the LBP value $LBP(x, y)$ (Fig. 2 c). Thus

$$LBP(x, y) = \sum_{k=0}^{7} s(i_k - i_c)^2 \tag{2}$$

where i_c is the intensity value of the center pixel (x,y), i_k is the intensity value of the 8 surrounding pixels, and function $s(x)$ is defined as:

$$s(x) = \begin{cases} 1 & \text{si } x \geq 0 \\ 0 & \text{si } x < 0 \end{cases} \tag{3}$$

The original formulation of the LBP was extended by Ojala [15] to consider a circular neighborhood instead of the 3x3 window. This circular neighborhood is defined by its radius R and the number of equally spaced pixels on that circle to compute the value of the LBP operator. The notation for this operator is $LBP_{P,R}$ being R the radius and P the number of pixels. $LBP_{8,1}$ and $LBP_{8,2}$ are shown in Figure 3.

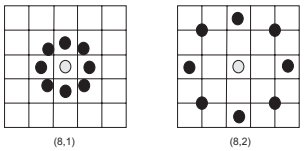

Figure 3. LBP operators for circular neighborhood

To test if LBP can be used as a focus measure it is necessary to test if it fulfills the properties that characterized the focus measures. This properties can be enumerate [20] as:

- *Unimodality*. A focus measure should be unimodal with only one maximum which must corresponds to the focus position where the image is focused.
- *Monotonicity*. The focus measure should exhibit an monotonous behavior on both side of the maximum, so the focus measure will have a different value for each focus position.
- *Defocus and noise sensibility* The ideal focus measure must only be dependent of the defocus and not to the noise in the image, but this is very difficult because as was mentioned focus measures are based on the amount of high frequencies with are also in the noise.
- *Effective range* It can be considered the range of focus positions where the focus measure maintains a sensitivity, in other words, the range where the focus measure fulfills the monotonicity property.
- *Computational efficiency* As many autofocus methods are intended to be used in consumer electronics, it is desirable that the computational requirements were low.
- *Robustness* This property implies that focus measures should yields the same results for the same defocus degree in different environmental conditions like illumination.

As it was stated in Section 1, defocus image can be modeled as a low-pass filtering process using a two-dimensional Gaussian PSF,

$$h(x, y) = \frac{1}{2\pi\sigma^2} \exp -\frac{x^2 + y^2}{2\sigma^2} \tag{4}$$

where σ is the standard deviation which corresponds to the spread of the PSF, so as σ increase the Gaussian filter behaves like a mean filter because the filter is more flattened. Therefore a defocus image will have less number of gray levels than a focus one. In the limit, a defocus image is a uniform gray image.

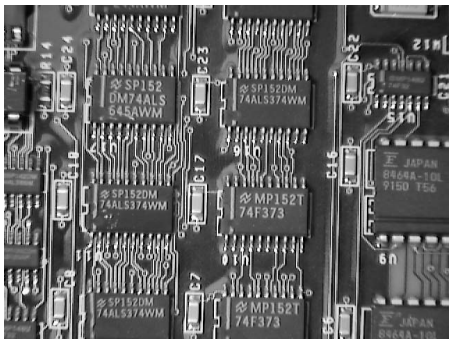

Figure 4. Test image

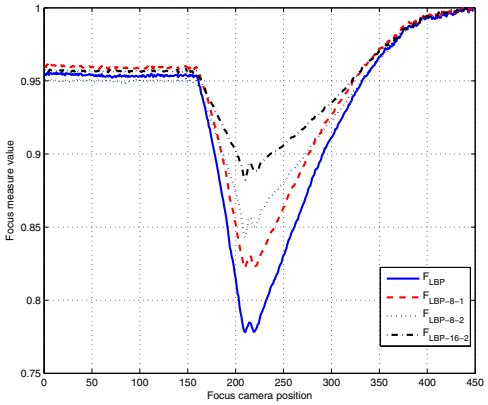

Figure 5. Results of the LBP based focus measures for the PCB images

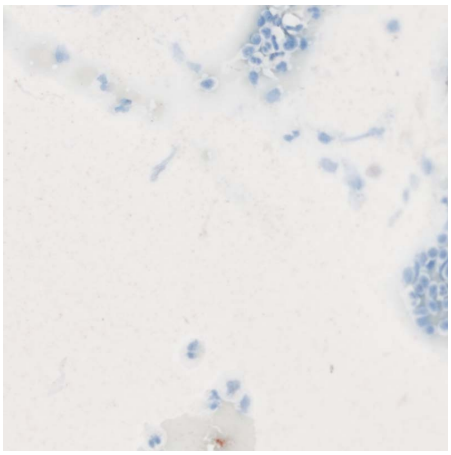

Figure 6. Microscope image

According to the definition of the LBP operator, its response to a defocus image will be higher than to a focus image because in the neighborhood of a pixel there are more pixels with the same intensity value and they contribute to the LBP value. In the LBP operator the contribution of each pixel in the neighborhood depends on its relative position to the center which is important to capture textures and so. However, in a focus measure the geometrical information is not important and only the existence of intensity differences between the central pixels and its surroundings must be taken into account. Thus in our application of the LBP as a focus measure, the weights are set to 1 and the original LBP operator turns into the count of pixels that has a higher or equal intensity value than the central pixel. Thus, the overall image focus measure F_{LBP} is defined as:

$$F_{LBP} = \sum_{i,j} LBP_{constant}(i,j) \tag{5}$$

where $LBP_{constant}(i,j)$ is the LBP operator computed on the 3x3 neighborhood centered at pixel i,j with constant weights,

$$LBP_{constant}(x,y) = \sum_{k=0}^{7} s(i_k - i_c) \tag{6}$$

To assess the previous assumptions about the behavior of the LBP operator as a focus measure, a test is carried out in a test image (Fig. 4), where a set of 448 images of the PCB were taken at different positions of the camera focus. Four versions of the LPB operator with constant weights were compared: F_{LBP}, $F_{LBP-8-1}$, $F_{LBP-16-1}$ and $F_{LBP-16-1}$. The normalized focus curves for the previous measures are shown in Figure 5. It is observed that the four proposed focus measures exhibit a monotonous behavior because they yields the minimum value when the image is focus and they increase their values when the image defocus. Although the four proposed measures fulfill the unimodality and monotonocity properties, F_{LBP} is the measure with the largest difference between its minima and maxima values. An important remark is that the images correspond to a real PCB so the letters in the chips are closer to the camera than the traces and this is the reason why the curves exhibit two minima: one minimum when the letters are correctly focus and the second minimum when the traces of the PCB are correctly focus.

In order to test the proposed focus measures in another scenario, the same comparison was carried out with a set of images taken with a microscope (Fig. 6). In this case, the proposed focus measures only exhibit one minimum because the preparation is flat (glass slide) and the unimodality and monotonocity properties can be observed more clearly than with the PCB images (Fig. 7). Unlike PCB images, the measure with the largest range is $F_{LBP-8-2}$ and it can be due to the geometry of the elements that appear in each image. In the PCB images, the letters and traces have many

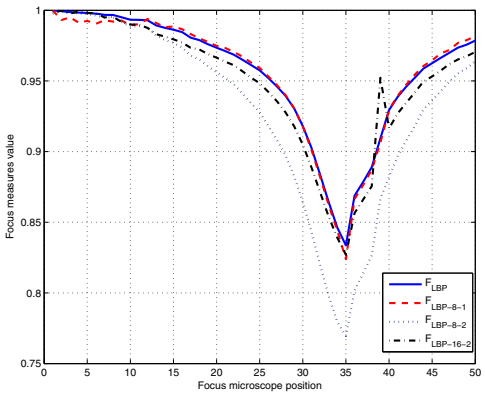

Figure 7. Results of the LBP based focus measures for the microscope images

square corners but in the microscope images the cells are rounded so a circular neighborhood is best fit.

3 Focus Measures

In this section, some well known focus measures are briefly described to compare with the proposed focus measures based on the LBP operator. The Tenenbaum Gradient (Tenengrad) [5] was one of the first proposed focus measures. This measure convolves the image with vertical (S_x) and horizontal (S_y) Sobel operators. To get a global measure over the whole image, the square of the gradient vector components are summed.

$$F_{Tenengrad} = \sum\sum S_x(x,y)^2 + S_y(x,y)^2 \qquad (7)$$

The Sum of Modified Laplace (SML) [13] is based on the linear differential operator Laplacian which has the same properties in all directions and is therefore invariant to rotation. Thus, the SML measure sums the absolute values of the convolution of the image with the Laplacian operators.

$$F_{SML} = \sum\sum |L_x(x,y)| + |L_y(x,y)| \qquad (8)$$

Energy Laplace [18] is based on the same idea of the SML measure but the image is convolved with the following mask,

$$L = \begin{bmatrix} -1 & -4 & -1 \\ -4 & 20 & -4 \\ -1 & -4 & -1 \end{bmatrix}$$

which computes the second derivate $D(x,y)$ of the image. The value of the focus measure is the sum of the squares of the convolution results.

$$F_{EnergyLaplace} = \sum\sum D(x,y)^2 \qquad (9)$$

Figure 8. Face image

Nanda and Cutler [11] proposed a focus measure from the contrast of a image as the absolute difference of a pixel with its eight neighbors, summed over all the pixels of the image.

$$F_{Contrast} = \sum\sum C(x,y) \qquad (10)$$

where the contrast $C(x,y)$ for each pixel in the gray image $I(x,y)$ is computed as

$$C(x,y) = \sum_{i=x-1}^{x+1} \sum_{j=y-1}^{y+1} |(I(x,y) - I(i,j)|$$

4 Experiments

Three different images will be used in these experiments: the PCB images, the microscope images and images corresponding to a typical human-computer interaction scenario (Fig, 8). The latter has as distinctive feature that the face is not a planar object so the measures will not show a clear peak that matches with the image completely focus. Of the proposed measures only F_{LBP} and $F_{LPB-8-2}$ will be utilized in the comparison because they showed the best performance.

Figure 9 shows the results obtained in the PCB set of images. The gradient based focus measures give sharper peaks than the two proposed measures and all of them have similar performance. However they only show one peak without taking into account the existence of two different planes with different distances to the camera where elements of interest appear (letters and traces).

Figure 10 shows the results obtained for the microscope images. As it was previously stated, $F_{LBP-8-2}$ exhibits better results than F_{LBP}. With respect to the other measures, Tenengrad and Energy Laplace do not show a well shaped peak so their performance is worse than the LBP based measures. On the other hand, SML and the measure proposed by Nanda give similar results with a larger range than the one proposed in this work.

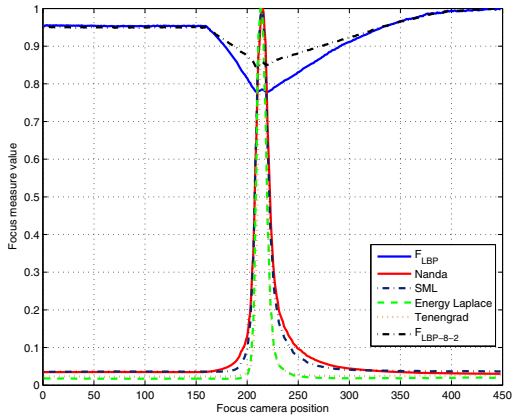

Figure 9. Normalized curves for the PCB images

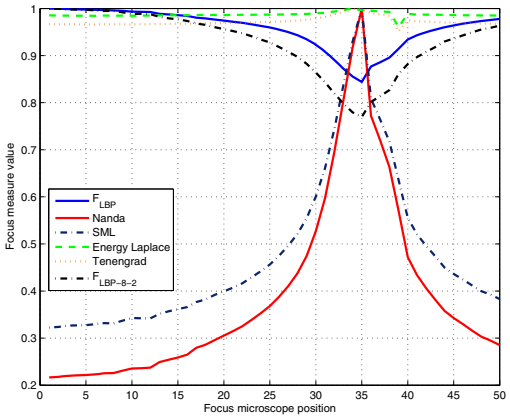

Figure 10. Normalized curves for the microscope image

Finally, the test was carried out in a more challenging scenario like human-computer interaction where the face is not flat and other elements appear in the image at different distances from the camera. Results are show in Figure 11 where it can be observed that this is the worst scenario for the proposed measures because they do not show any peak and it is difficult to focus a camera in this situation. For the rest of the measures in the comparison, the results are very similar results so they are more suitable for this kind of scenarios where the objects that appear in the image are not at the same distance from the camera.

After the previous analysis, the focus positions that give the peak in the focus curve are computed (Table 1). In the PCB image, the focus position for F_{LBP} and $F_{LBP-8-2}$ is 210 whereas for the other measures is 215. However, F_{LBP} and $F_{LBP-8-2}$ also have a peak at position 219, so the other measures yields a peak that is located between the two peaks of the proposed measures. For the microscope image all the measures reach its optimum at position of 35 except for Tenengrad and Energy Laplace that reach the maximum at position 34 but they do not show a clear peak (Fig. 10). Finally, the analysis for the HCI image reveal that there is a disparity in the position of the peak for the compared measures although all except F_{LBP} and $F_{LBP-8-2}$ give a good peak. From this analysis of peak position, it can be concluded that for planar scenarios the measures proposed in this work gives similar positions to the ones given by the other measures.

5 Conclusions

In this work the use of LBP operators as a focus measure has been studied. Four LPB based focus measures have been defined based on their equivalent LBP operators. To assess their performance as a focus measures there were used as testbed two set of images. In the first set of images (PCB) the best performance was achieved by the measure F_{LBP}, whereas the measure $F_{LBP-8-2}$ gives better performance in the second set of images (microscope). This can be due to the geometry of the images elements, with square corners in the first set and rounded in the second set. In both cases all the proposed measures fulfill the unimodality and monotonicity properties but there exists difference in the range of values, giving one of them a more sharp peak than the others.

In order to know how good are the proposed measures, a comparison with five well know focus measures was carried out. The tests were realized with three set of images and as conclusion the F_{LBP} and $F_{LBP-8-2}$ gives good results in planar scenes like the PCB and microscope images but it has a bad performance in scenes where elements in the scene appear at different distance from the camera as in human-computer interaction.

As future work, some experiments must be realized in other to test the robustness to noise and illumination changes in the image. Also, new LBP operators as those that are rotation invariant or uniform ones can be included in the study to test if they introduce some improvements over the results obtained with the operators proposed in this work.

Acknowledgements

Thanks to Gloria Bueno for providing the microscopy set of images, and projects PAI08-0283-9663 of the Junta de Comunidades de Castilla-La Mancha and ULPGC07-008 of

Table 1. Focus position of maximum (minimum) value for each measure

	$F_{LBP-8-1}$	$F_{LBP-8-2}$	Tenengrad	SML	Energy Laplace	Nanda
PCB image	210	210	215	215	215	215
Microscope image	35	35	34	35	34	35
HCI image	259	258	385	353	385	353

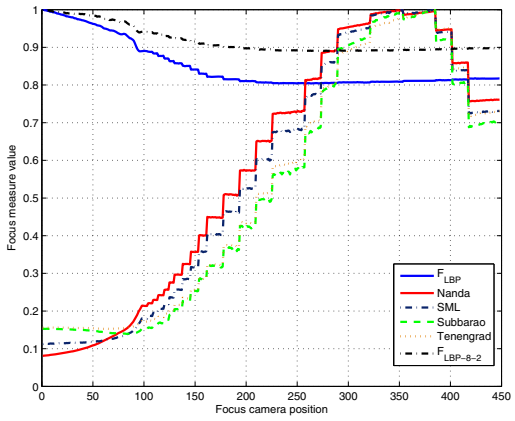

Figure 11. Normalized curves for the face image

the University of Las Palmas de Gran Canaria that partially funded this work.

References

[1] T. Ahonen, A. Hadid, and M. Pietikinen. Face description with local binary patterns: Application to face recognition. *IEEE Transactions on Pattern Analysis and Machine Intelligence*, 28(12):2037–2041, December 2006.

[2] D. Hansen and A. Pece. Iris tracking with feature free contours. In *IEEE International Workshop on Analysis and Modeling of Faces and Gestures (AMFG 2003)*, pages 208–214, 2003.

[3] N. Kehtarnavaz and H.-J. Oh. Development and real-time implementation of a rule-based auto-focus algorithm. *Real-Time Imaging*, 9:197–203, 2003.

[4] M. Kristan, J. Pers, M. Perse, and S. Kovacic. A bayes-spectral-entropy-based measure of camera focus using a discrete cosine transform. *Pattern Recognition Letters*, 27(13):1419–1580, October 2006.

[5] E. Krotkov. Focusing. *International Journal of Computer Vision*, 1:223–237, 1987.

[6] S. Kuiper and B. Hendriks. Variable-focus liquid lens for miniature cameras. *Applied Physics Letters*, 85:1128–1130, 2004.

[7] J.-H. Lee, K.-S. Kim, and B.-D. Nam. Implementation of a passive automatic focusing algorithm for digital still camera. *IEEE Transactions on Consumer Electronics*, 41(3):449–454, 1995.

[8] J.-S. Lee, Y.-Y. Jung, B.-S. Kim, and K. Sung-Jea. An advanced video camera system with robust AF,AE and AWB control. *IEEE Transactions on Consumer Electronics*, 47(3):694–699, August 2001.

[9] S. Marcel, Y. Rodriguez, and G. Heusch. On the recent use of local binary patterns for face authentication. *International Journal on Image and Video Processing Special Issue on Facial Image Processing*, 2007.

[10] C. H. Morimoto and M. R. Mimica. Eye gaze tracking techniques for interactive applications. *Computer Vision and Image Understanding*, 98(1):4–24, April 2005.

[11] H. Nanda and R. Cutler. Practical calibrations for a real-time digital onmidirectional camera. In *Proceedings of the Computer Vision and Pattern Recognition Conference (CVPR 2001)*, 2001.

[12] N. Nathaniel, P. Neow, and M. Ang. Practical issues in pixel-based autofocusing for machine vision. In *Proc. of the 2001 IEEE International Conference on Robotics and Automation*, Seoul, Korea, May 21-26 2001.

[13] Y. Nayar, Shree K.and Nakagawa. Shape from focus. *IEEE Transactions on Pattern Analysis and Machine Intelligence*, 16(8):824–831, August 1994.

[14] T. Ojala, M. Pietikinen, and D. Harwood. A comparative study of texture measures with classification based on featured distributions. *Pattern Recognition*, 29(1):51–59, January 1996.

[15] T. Ojala, M. Pietikinen, and T. Menp. Multiresolution gray-scale and rotation invariant texture classification with local binary patterns. *IEEE Transactions on Pattern Analysis and Machine Intelligence*, 24(7):971–987, july 2002.

[16] R. K. Park and J. Kim. A real-time focusing algorithms for iris camera recognition. *IEEE Transactions on Systems, Man and Cybernetics*, 35(3):441–444, August 2005.

[17] M. Shirvaikar. An optimal measure for camera focus and exposure. In *Proceedings of the Thirty-Sixth Southeastern Symposium on System Theory*, pages 472– 475, 2004.

[18] M. Subbarao and J.-K. Tyan. Selecting the optimal focus measure for autofocusing and depth-from-focus. *IEEE Transactions on Pattern Analysis and Machine Intelligence*, 20(8):864–870, August 1998.

[19] Z. Sun, T. Tan, and X. Qiu. Graph matching iris image blocks with local binary pattern. In *Advances in Biometrics: International Conference, ICB 2006*, volume 3832 of *Lecture Notes in Computer Science*, pages 366–372, 2006.

[20] Y. Tian, K. Shieh, and C. Wildsoet. The performance of focus measures in the presence of non-defocus aberrations. *Journal of the Optical Society of America A*, 2007.